Structure and evolution of galaxies at z~1

Janusz Krywult[1], Agnieszka Pollo[2,3] and The VIPERS Team[4]

1. Institute of Physics, Jan Kochanowski University, Swietokrzyska 15, 25–406 Kielce, Poland
2. Astronomical Observatory, Jagiellonian University, Orla 171, 30–001 Kraków, Poland
3. National Center for Nuclear Research, A. Sołtana 7, 05–400 Otwock, Poland
4. The VIPERS Team coauthors are presented at the end of this proceedings

Using the spectroscopic and photometric data from the VIPERS, together with the CFHTLS images we found that early-type galaxies display only a slow change of their concentrations with cosmic time since $z \sim 1$ epoch. It is already established by $z \sim 1$ and depends much more strongly on their luminosities. In contrast, late-type galaxies get clearly more concentrated with cosmic time since $z \sim 1$, with only little evolution in colour, which remains dependent mainly on their luminosity.

1 Introduction

In Hubble's classification, today's early-type galaxies are usually redder in optical colours, more luminous and massive, with older stellar populations, and smaller reservoirs of gas and dust; conversely, late-type galaxies are generally less massive, show younger stellar populations and have bluer colours. The standard approach to study the galaxy structure and evolution is to identify a series of parameters which correlate with the visual morphology of a galaxy and to define the parameter–space which best identifies a specific morphological type. A widely used parametric description of the galaxy light profile is based on the exponent n of the Sérsic (1963) law which is fitted to the galaxy surface brightness distribution. Many studies have shown that the single Sérsic profile index $n \approx 2$ well separates early- and late-type galaxies (e.g. Driver et al., 2006). Similarly to what is seen in the Sérsic index distribution galaxy rest-frame, colours tend to segregate into a bimodal distribution in which two clear loci are preferentially occupied by the blue and the red populations, known respectively as the *blue cloud* and the *red sequence*.

The purpose of this work is to present a robust method to classify galaxies from intermediate redshift range to analyse their colour and morphological observational parameters from ground-based observations.

2 The data

In this study, we investigate the morphological properties of the VIPERS (VIMOS Public Extragalactic Redshift Survey) galaxies. VIPERS is an ESO Large Programme aimed at measuring redshifts for $\sim 10^5$ galaxies at $0.5 < z < 1.2$. The total area (about $24\,\mathrm{deg}^2$) and the depth of VIPERS result in a large volume, 5×10^7 h^{-3} Mpc^3. From the VIPERS observations, we selected only galaxies with highest redshift reliability, that is, with quality flag zflag = [2, 3, 4, 9]. Further details on the design of VIPERS data, along with its data products, can be found in Guzzo et al. (2014).

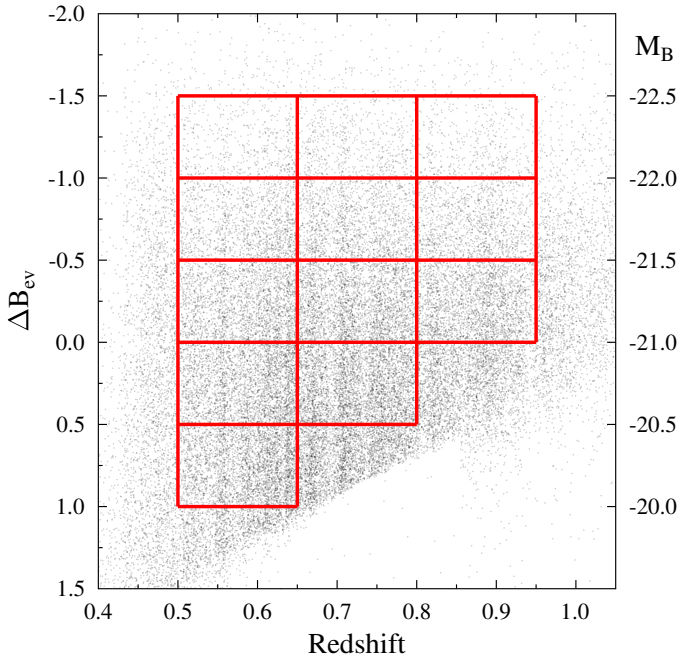

Fig. 1: Distribution of $B_{\rm ev}$ magnitue as a function of redshift. The red lines enclose the selected sub-samples of galaxies.

Photometric Data. The absolute magnitudes of the VIPERS galaxies were derived using the SED fitting as described in Fritz et al. (2014) study. To investigate the dependence of morphology and colour of galaxies on their redshift, we corrected their absolute magnitudes $M_{\rm B}$ to account for their intrinsic evolution. For this purpose, we used the global B-band luminosity function in the redshift range from $z = 0.5$ to 1.3 taken from Fritz et al. (2014) results. These data have been used for approximation of evolution with redshift characteristic magnitude M_* of the Schechter (1976) function, and to define the $B_{\rm ev}$ luminosity by the equation

$$\Delta B_{\rm ev} = M_{\rm B} + 19.90 + 1.59\,z. \quad (1)$$

Galaxy subsamples. Fig. 1 presents the distribution of the $\Delta B_{\rm ev}$ luminosity as a function of redshift. In this study, we considered 12 volume-limited subsamples represented by the red boxes in this plot. Each subsample is statistically complete, spans $\Delta B_{\rm ev} = 0.5$ magnitudes and has a redshift range $\Delta z = 0.15$. The left-side vertical axis shows the $\Delta B_{\rm ev}$ value, whereas the right-side axis gives the absolute magnitude $M_{\rm B}$ at the mean VIPERS redshift $z = 0.7$.

Galaxy morphology. The morphological analysis of $\sim 10^5$ VIPERS galaxies was based on the study of the surface brightness profile of these objects. To model the light profile of galaxies we used CCD images in the i-band from CFHTLS (Canada-France-Hawaii Telescope Legacy Survey) project, where the mean FWHM (full width at half maximum) is smallest and guarantees the secure quality of the derived morphological parameters. To derive the surface brightness parameters of galaxies, we have performed a 2D fit of the observed galaxy light distribution using GALFIT

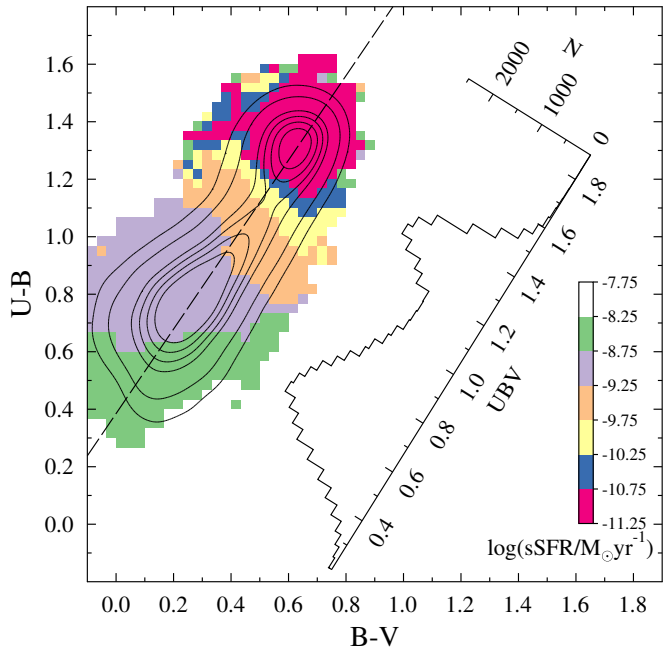

Fig. 2: $U-B$ versus $B-V$ colour diagram coded according to sSFR, and UBV colour histogram. Contours show the isodensity lines.

tool (Peng et al., 2002). We used the single component Sérsic (1963) profile given by the equation:

$$I(r) = I_{\rm e} \exp\left\{-b_{\rm n}\left[\left(\frac{r}{r_{\rm e}}\right)^{1/n} - 1\right]\right\}, \qquad (2)$$

where $r_{\rm e}$ is the radius enclosing half of the total light of the galaxy, $I_{\rm e}$ is the mean surface brightness at $r_{\rm e}$, and $b_{\rm n}$ is a normalization factor, which is chosen in such a way that $r_{\rm e}$ corresponds to the half-light radius. A full description of the data processing and statistical tests of the obtained results are provided in Krywult et al. (2017).

3 Galaxy UBV colour

To probe the colour distribution of VIPERS galaxies we used the rest-frame $(U-B)$ versus $(B-V)$ colour-colour plot. The isodensity contour lines presented in Fig. 2 show an evident bimodality in the rest-frame colours, with two well-separated peaks, which in the local Universe are known to be well correlated with the early and late galaxy Hubble types. We defined the combined colour UBV by projecting the galaxy rest-frame colours along the $A-A$ line that connects the two density peaks drawn in this figure. Moreover, Fig. 2 is colour coded by the median specific Star Formation Rate (sSFR) of galaxies. The correlation between the UBV colours and sSFR is therefore clearly evident, with blue colours corresponding to higher values of sSFR and red galaxies being mostly quiescent (Davidzon et al., 2016).

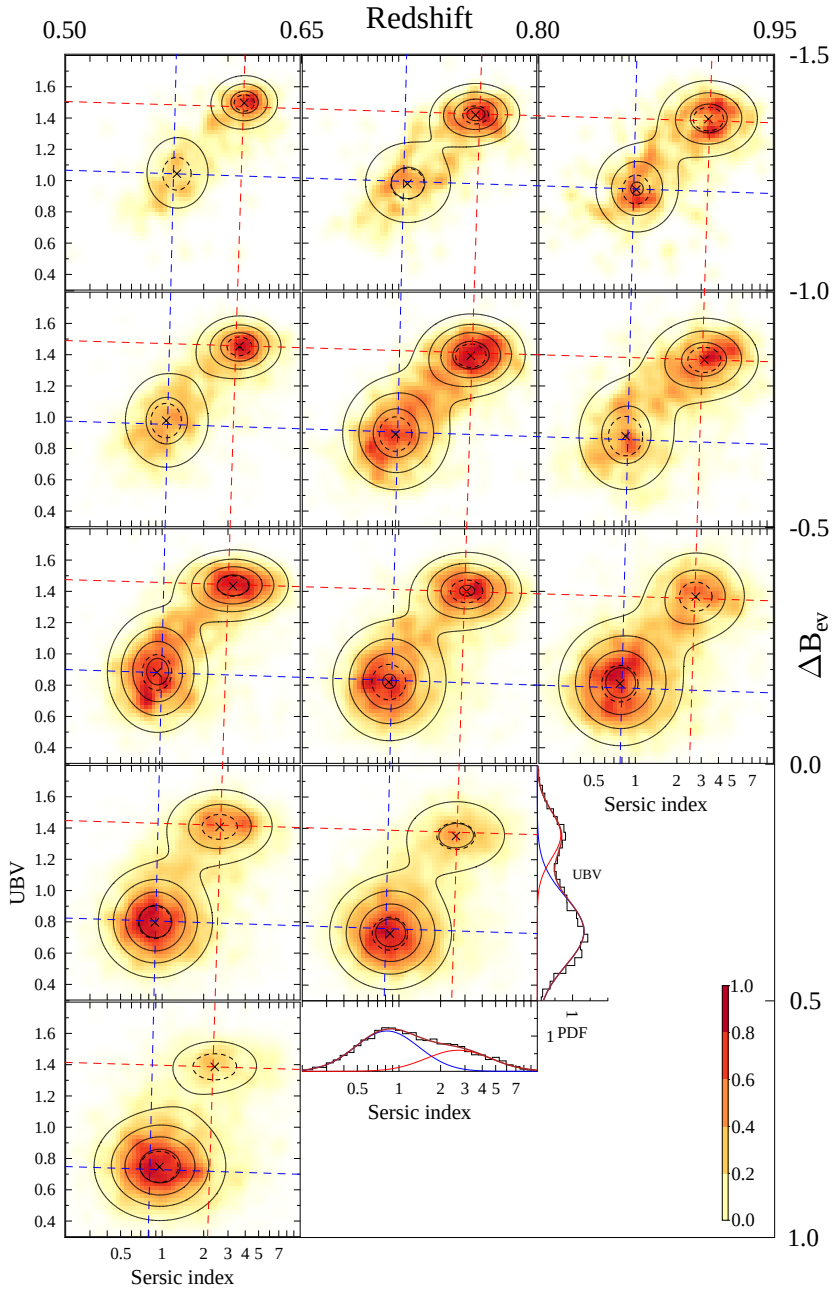

Fig. 3: UBV rest-frame colour vs Sérsic index n surface density maps. Each panel shows the colour coded galaxy surface density distribution map of the studied galaxies in each redshift and $B_{\rm ev}$ luminosity bin. The contour lines show the density values in steps of 0.2, obtained from the two Gaussians bivariate fitting procedure. Blue and red dashed lines show the 2-dimensional relations given by Eqs. 3 and 4 (Krywult et al., 2017).

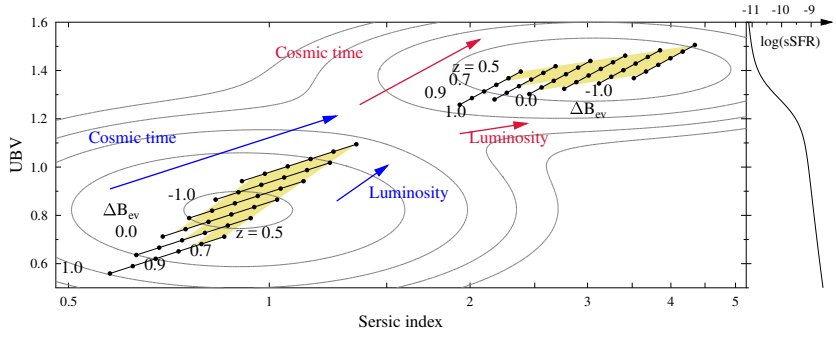

Fig. 4: UBV colour versus Sérsic index $\log(n)$ relation of late-type (lower left corner) and early-type (upper right corner) galaxies. Dots indicate redshift whereas solid black lines connect the fixed value of the $\Delta B_{\rm ev}$ luminosity. The arrows show the direction of the redshift and luminosity galaxy evolution. The right plot presents the $UBV(sSFR)$ relation. The background contour lines show the number density of all studied galaxies. The khaki coloured regions mark the analysed redshift and luminosity limits.

4 Sersic index – UBV colour distribution

Using the local galaxy sample of the Millennium Galaxy Catalogue, Driver et al. (2006) showed that two well-separated populations of galaxies exist on the $u-r$ rest-frame colour versus $\log(n)$ Sérsic index plane. Our study of VIPERS galaxies showed that the surface density maps of UBV rest-frame colour versus Sérsic index n presented in Fig. 3 are clearly bimodal in all panels, with two well-separated peaks and indicate the presence of two different populations that we identify with early- and late-type galaxies. We found that the distribution of the late-type galaxies are centered at the Sérsic index value $n \approx 1$ and the rest-frame colour $UBV \approx 0.8$, while those of the early-type galaxies are centered at $UBV \sim 1.4$ and $2.5 < n < 4$. Fig. 3 also shows that the most luminous bins are dominated by early-type galaxies, whereas the late-like galaxies dominate the less luminous sub-samples.

5 Sérsic index – UBV colour coevolution

The galaxy surface distributions presented in Fig. 3 show that marked by crosses the early- and late-type galaxy populations centres vary with both redshift and luminosity. Using these locations, we determined the empirical relation connecting the galaxy population centre (given by $\log(n), UBV$) with $\Delta B_{\rm ev}$ and redshift. We obtained the following set of equations describing the position of late- and early-type galaxy population centres as a functions of redshift z and luminosity
a) late-type galaxies

$$\log(n_{\rm l}) = 0.18 - 0.34z - 0.08\Delta B_{\rm ev}, \qquad UBV_{\rm l} = 1.02 - 0.31z - 0.15\Delta B_{\rm ev}, \quad (3)$$

b) early-type galaxies

$$\log(n_{\rm e}) = 0.57 - 0.18z - 0.10\Delta B_{\rm ev}, \qquad UBV_{\rm e} = 1.58 - 0.27z - 0.04\Delta B_{\rm ev}. \quad (4)$$

The functions given by Eqs. 3 and 4 are ploted in Fig. 3 as blue and red dashed lines, respectively. The empirically derived set of presented above equations describes the

coevolution of the UBV rest-frame colours and Sérsic indices and allows us to give a general overview of the colours and structural properties of late- and early-type galaxies. Fig. 4 shows explicitly the effect of evolution and luminosity on the colours and structural properties of both morphological types of galaxies.

Early-type galaxies. The study shows that the effects of increasing luminosity and cosmic time on early-type galaxies act in different directions. At $z = 1.0$, we see that a low-luminosity ($\Delta B_{\rm ev} = +1.0$) red galaxy is 0.10 mag bluer in UBV, and 0.6 times less concentrated than its 10 times more luminous ($\Delta B_{\rm ev} = -1.5$) red counterpart. Following a galaxy evolutionary track, we see that while a galaxy can rapidly redden to match its high-luminosity counterpart by $z = 0.63$, over the same time-scale it only marginally increases its concentration by a factor equal to 1.17, i.e. only a quarter of the amount needed to match that of high-luminosity early-type galaxies at $z = 1.0$. Indeed, even at $z = 0$ (assuming an extrapolation of the linear trends) its Sérsic index will not have increased sufficiently.

Late-type galaxies. The concentration of late-type galaxies is most dependent on cosmic time, while UBV colour increases mostly with luminosity. At $z = 1.0$, a low-luminosity late-type galaxy ($\Delta B_{\rm ev} = +1.0$) is 0.375 mag bluer and 1.6 times less concentrated than its 10 times more luminous counterpart ($\Delta B_{\rm ev} = -1.5$). By following its evolutionary track, it is able to change its structure sufficiently rapidly to match the Sérsic index of its high-luminosity counterpart by $z = 0.41$, but over the same time period it is only expected to become 0.18 mag redder, half of that required to match the UBV colour of the high-luminosity late-type galaxies at $z = 1$.

6 Conclusions

The combination of the UBV rest-frame colour and Sérsic index n as a function of redshift and luminosity allows to study coevolution of these properties of galaxies over the redshift range from $z = 1$ to 0.5. We found the evident and consistent bimodality in the UBV rest-frame colour and Sérsic index distribution up to redshift $z = 1$. The study shows that the early-type galaxies display only a slow change of their concentration since $z \sim 1$; it is already established by $z \sim 1$ and depends much more strongly on their luminosities. The late-type galaxies get clearly more concentrated with cosmic time since $z \sim 1$, with only a little evolution in colour, which remains dependent mainly on their luminosity.

Acknowledgements. We acknowledge the support from the Polish National Science Centre grants No. UMO-2012/07/B/ST9/04425 and UMO-2013/09/D/ST9/04030. Funding for VIPERS has been provided by the PRIN-INAF 2008 grant "VIMOS Public Extragalactic Redshift Survey (VIPERS): the large scale structure and growth rate of the Universe at $z\,1$ from a survey of 100,000 galaxy redshifts".

References

Davidzon, I., et al., *A&A* **586**, A23 (2016)
Driver, S. P., et al., *MNRAS* **368**, 414 (2006)
Fritz, A., et al., *A&A* **563**, A92 (2014)
Guzzo, L., et al., *A&A* **566**, A108 (2014)
Krywult, J., et al., *A&A* **598**, A120 (2017)

Peng, C. Y., Ho, L. C., Impey, C. D., Rix, H.-W., *AJ* **124**, 266 (2002)

Schechter, P., *ApJ* **203**, 297 (1976)

Sérsic, J. L., *Boletin de la Asociacion Argentina de Astronomia La Plata Argentina* **6**, 41 (1963)

[1]The VIPERS Team coauthors: U. Abbas[5], C. Adami[4], S. Arnouts[6], J. Bel[7], M. Bolzonella[9], D. Bottini[3], E. Branchini[10·28·29], A. Cappi[9], J. Coupon[12], O. Cucciati[9], I. Davidzon[9·17], G. De Lucia[13], S. de la Torre[14], A. Fritz[3], P. Franzetti[3], M. Fumana[3], B. Garilli[3·4], B. R. Granett[2], L. Guzzo[2·27], O. Ilbert[4], A. Iovino[2], V. Le Brun[4], O. Le Fèvre[4], D. Maccagni[3], K. Małek[16·3], F. Marulli[17·18·9], H. J. McCracken[19], L. Paioro[3], M. Polletta[3], H. Schlagenhaufer[24·20], M. Scodeggio[3], L. A. .M. Tasca[4], R. Tojeiro[11], D. Vergani[25·9], A. Zanichelli[26], A. Burden[11], C. Di Porto[9], A. Marchetti[1·2], C. Marinoni[7], Y. Mellier[19], L. Moscardini[17·18·9], R. C. Nichol[11], J. A. Peacock[14], W. J. Percival[11], S. Phleps[20], M. Wolk[19], G. Zamorani[9] [1] Università degli Studi di Milano; [2] INAF - Osservatorio Astronomico di Brera; [3] INAF - Istituto di Astrofisica Spaziale e Fisica Cosmica Milano; [4] Aix Marseille Université, CNRS, LAM (Laboratoire d'Astrophysique de Marseille); [5] INAF - Osservatorio Astronomico di Torino; [6] Canada-France-Hawaii Telescope; [7] Centre de Physique Théorique, UMR 6207 CNRS-Université de Provence; [8] Université de Lyon; [9] INAF - Osservatorio Astronomico di Bologna; [10] Dipartimento di Matematica e Fisica, Università degli Studi Roma Tre; [11] Institute of Cosmology and Gravitation, Dennis Sciama Building, University of Portsmouth; [12] Institute of Astronomy and Astrophysics, Academia Sinica; [13] INAF - Osservatorio Astronomico di Trieste; [14] SUPA, Institute for Astronomy, University of Edinburgh, Royal Observatory; [15] Department of Particle and Astrophysical Science, Nagoya University; [16] Dipartimento di Fisica e Astronomia - Università di Bologna; [17] INFN, Sezione di Bologna; [18] Institute d'Astrophysique de Paris, UMR7095 CNRS, Université Pierre et Marie Curie; [19] Max-Planck-Institut für Extraterrestrische Physik; [20] Universitätssternwarte München, Ludwig-Maximillians Universität; [21] INAF - Istituto di Astrofisica Spaziale e Fisica Cosmica Bologna; [22] INAF - Istituto di Radioastronomia; [23] Dipartimento di Fisica, Università di Milano-Bicocca; [24] INFN, Sezione di Roma Tre; [25] INAF - Osservatorio Astronomico di Roma